NACA RM L55I26

CASE FILE
COPY

NACA

RESEARCH MEMORANDUM

LATERAL-CONTROL INVESTIGATION AT TRANSONIC SPEEDS

OF DIFFERENTIALLY DEFLECTED HORIZONTAL-TAIL

SURFACES FOR A CONFIGURATION HAVING A

6-PERCENT-THICK 45° SWEPTBACK WING

By Chris C. Critzos

Langley Aeronautical Laboratory
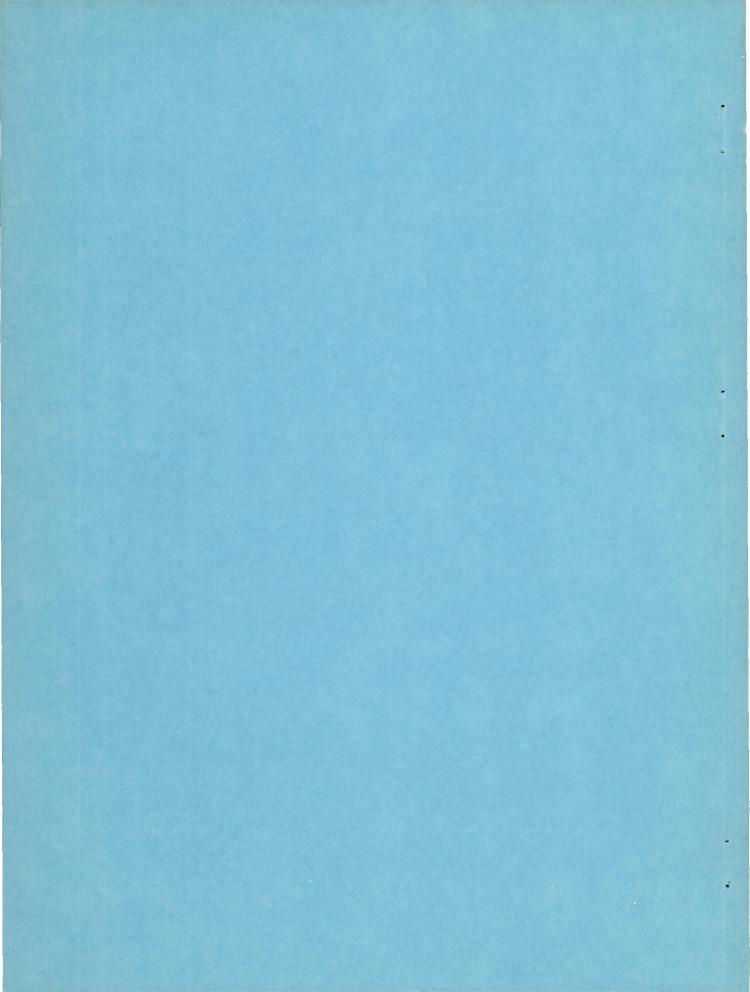Langley Field, Va.

Aircraft Armaments, Inc.
Cockeysville, Maryland

NATIONAL ADVISORY COMMITTEE
FOR AERONAUTICS

WASHINGTON
November 15, 1955

NATIONAL ADVISORY COMMITTEE FOR AERONAUTICS

RESEARCH MEMORANDUM

LATERAL-CONTROL INVESTIGATION AT TRANSONIC SPEEDS

OF DIFFERENTIALLY DEFLECTED HORIZONTAL-TAIL

SURFACES FOR A CONFIGURATION HAVING A

6-PERCENT-THICK 45° SWEPTBACK WING

By Chris C. Critzos

SUMMARY

An investigation has been conducted in the Langley 16-foot transonic tunnel to determine the lateral-control effectiveness of differentially deflected horizontal-tail surfaces mounted behind a 45° sweptback wing-fuselage combination. Both the wing and the horizontal tail had an aspect ratio of 4.0, a taper ratio of 0.6, and NACA 65A006 airfoil sections parallel to the plane of symmetry. The ratio of the span of the horizontal tail to the span of the wing was 0.427. Force data were obtained for the basic tail-off configuration and for horizontal-tail surfaces mounted at an angle of symmetrical incidence of -4°. Data were also obtained for the horizontal tail at an angle of differential incidence of 20° with and without the vertical tail. The Mach number ranged from 0.80 $\left(\text{Reynolds number of } 5.4 \times 10^6\right)$ to 1.05 $\left(\text{Reynolds number of } 6.4 \times 10^6\right)$ for an angle-of-attack range of approximately 0° to 20°.

The effectiveness of the differentially deflected horizontal tail as a lateral-control device was found to be essentially independent of angle of attack and Mach number even in the transonic region. The rolling-moment coefficient C_l showed about 15-percent variation from a value of about 0.0075 except at a Mach number of 0.94. At a wing angle of attack of 2°, the rolling-moment effectiveness of the horizontal tail deflected differentially corresponded to that for a 30-percent midspan aileron at a total deflection of about 6° for Mach numbers up to 0.96 and to as high as 15° at Mach numbers between 0.96 and 1.05. Considerable favorable yawing moment was indicated at low angles of attack and the yawing moment decreased appreciably at higher angles of attack. Removing the vertical tail had negligible effect on rolling moment, although the yawing-moment and lateral-force changes were significant.

INTRODUCTION

The loss of effectiveness of conventional flap-type ailerons at high subsonic and at supersonic speeds has necessitated the consideration of other lateral-control devices with more favorable high-speed characteristics. At present, other types of control being investigated for use at high speeds include spoilers and differentially deflected horizontal-tail surfaces. The effectiveness of spoilers as lateral-control devices at subsonic and supersonic speeds has been previously reported (for example, refs. 1 and 2). However, although data are presently available on the lateral-control effectiveness of differentially deflected horizontal-tail surfaces at low speeds (refs. 3 and 4) very little data (ref. 5) exist for high subsonic and supersonic speeds. To obtain additional information on the applicability of differentially deflected horizontal tails as high-speed lateral-control devices, a short investigation has been conducted in the Langley 16-foot transonic tunnel of the effectiveness of a horizontal tail deflected differentially $\pm 10^\circ$ from a constant mean angle of incidence behind a 6-percent-thick-sweptback wing over a Mach number range from 0.80 to 1.05.

This paper presents the rolling-moment effectiveness obtained for the differentially deflected horizontal tail and includes a comparison with flap-type ailerons. The effect of the vertical tail on the rolling-moment effectiveness of the horizontal tail is also evaluated.

SYMBOLS

All coefficients are referred to the stability system of axes with the origin at the quarter-chord of the mean aerodynamic chord.

b wing span

c local wing chord

$\bar{c}$ wing mean aerodynamic chord

C_D drag coefficient, Drag/qS

C_L lift coefficient, Lift/qS

C_l rolling-moment coefficient, Rolling moment/qSb

C_m pitching-moment coefficient, Pitching moment/$qS\bar{c}$

C_n yawing-moment coefficient, Yawing moment/qSb

C_Y lateral-force coefficient,   Lateral force/qS

M free-stream Mach number

P_b base pressure coefficient, $\dfrac{p_b - p_o}{q}$

p_b static pressure at base of model

p_o free-stream static pressure

q free-stream dynamic pressure

R Reynolds number, based on $\bar{c}$

r fuselage radius

S total wing area

x longitudinal distance, positive rearward of fuselage nose

α angle of attack of fuselage center line relative to air flow

ΔC_l, ΔC_n, ΔC_Y incremental coefficients produced by addition of or changes in deflection of control surfaces

APPARATUS

Tunnel

The tests for the present investigation were conducted in the Langley 16-foot transonic tunnel, a single-return octagonal slotted-throat wind tunnel. A detailed description of this tunnel is presented in reference 6. As indicated in this reference, the maximum variation of the average Mach number along the test-section center line in the vicinity of the model is about ±0.002.

Model

The wing-fuselage combination used in the present investigation was similar, except for fuselage dimensions, to that used for a general research program on a 45° sweptback wing-body combination at transonic speeds (see refs. 1 and 7). The aluminum-alloy wing had NACA 65A006 airfoil sections parallel to the airstream, 45° sweepback of the quarter-chord line, a taper ratio of 0.6, and an aspect ratio of 4.0. Ordinates for the NACA 65-A series airfoil sections may be found in reference 8.

CONFIDENTIAL

The wing was mounted in a midwing position on the fuselage and had no geometric incidence, dihedral, or twist. The fuselage consisted of a cylindrical body of revolution, an ogival nose, and a slightly boattailed afterbody. The fineness ratio of the fuselage was 10.95 and the ratio of the base diameter to the maximum diameter was 0.66. The horizontal tail was geometrically similar to the wing and was mounted in the midfuselage position. The ratio of the span of the horizontal tail to the span of the wing was 0.427. For symmetrically deflected tail-surface tests the angle of incidence was -4° and for differentially deflected tail-surface tests, the tail surfaces were deflected $\pm 10^\circ$ from a constant mean angle of incidence of -4°. The horizontal tail was bolted to the fuselage and all gaps were filled and faired smooth for each tail-on configuration. The geometric details of the model, including a table of fuselage ordinates, are given in figure 1. A photograph of the model mounted in the Langley 16-foot transonic tunnel is shown in figure 2.

Model Support System

A single swept cantilever strut supported the sting-mounted model for the present tests. This support system, described in detail in reference 7, held the model near the tunnel center line throughout the angle-of-attack range. A 5° coupling between the sting and the model permitted variations in the angle from 0° to 20°.

TESTS

The present investigation consisted of measuring the aerodynamic forces and moments for each model configuration through a wide angle-of-attack range at Mach numbers of 0.80, 0.90, and 0.94. The maximum angle of attack was limited by wing root stresses to 20°, 16°, and 14°, respectively, for Mach numbers of 0.80, 0.90, and 0.94. At Mach numbers of 0.96, 0.98, 1.00, 1.03, and 1.05 data were generally obtained only up to 10° angle of attack.

Forces and moments were measured by a six-component electrical strain-gage balance mounted within the fuselage.

The Reynolds number for the present tests, based on a mean-aerodynamic-chord length of 1.531 feet, ranged from 5.4×10^6 to 6.4×10^6. The variation of Reynolds number over the speed range is presented in figure 3.

CONFIDENTIAL

CONFIDENTIAL

CORRECTIONS AND PRECISION

Force-Data Accuracy

The data presented herein were not adjusted for sting and tunnel-wall effects since these effects are known to be generally negligible within the present Mach number range. Neglecting these possible sources of small error, the accuracy of the force and moment coefficients, based on balance accuracy and repeatability of data, is believed to be within the following limits:

C_L . . . . ±0.01

C_D at low lift coefficients . . . . ±0.002

C_D at high lift coefficients . . . . ±0.004

C_m . . . . ±0.003

C_l . . . . ±0.001

C_n . . . . ±0.001

C_Y . . . . ±0.002

Angle of Attack

The model angles of attack relative to the tunnel center line were obtained by use of a pendulum-type strain-gage inclinometer mounted within the model and were corrected for tunnel flow angularity. Based on repeatability of data, the estimated maximum error in angle-of-attack measurements is ±0.1°.

Base Pressure

Lift and drag data were adjusted to the condition of free-stream static pressure at the model base. The variations of the base pressure for all configurations which were measured by three orifices located 2 inches inside the base of the model are presented as functions of angle of attack for the Mach numbers of the present investigation in figure 4. Repeat points obtained for the differentially deflected vertical-tail-on configuration indicated a maximum scatter in the base pressure coefficient of 0.014 occurring at M = 1.00 and α = 10°, which amounted to a drag-coefficient increment of approximately 0.0003.

CONFIDENTIAL

RESULTS AND DISCUSSION

Data obtained in the present investigation for the basic tail-off configuration and for the symmetrical tail-on configuration are presented without discussion in figures 5 and 6. Figures 7 and 8 compare the effects of differentially deflecting the two halves of the tail surfaces and of removing the vertical tail. Figure 9 presents the incremental lateral forces and moments resulting from deflecting the tail surfaces differentially with and without the vertical tail. Figure 10 presents the deflection of a 30-percent-chord aileron which will produce the same rolling moment as the differentially deflected horizontal tail.

Effects of Differential Deflection of

Horizontal-Tail Surfaces

Rolling-moment coefficient.- Lateral-control effectiveness of the differential tail showed little variation with angle of attack and Mach number, and agrees in this respect with the data of reference 5. This effectiveness was essentially constant with angle of attack at a value approximately 0.007 at the lower Mach numbers, except at Mach number of 0.94 for a small angle-of-attack range, and increased to about 0.009 at Mach numbers of 1.03 and 1.05 (figs. 7(c) and 9(a)).

Figure 10 presents the deflection (obtained by interpolation of data of ref. 9) required of a 30-percent-chord flap-type aileron to produce approximately the same rolling moment as the differentially deflected horizontal tail of the present tests. These deflections were obtained for a 0.43-semispan aileron located outboard on a semi-span reflection-plane model that was smaller but geometrically similar to the model of the present tests. The equivalent deflection of the single aileron at an angle of attack of 2^O was about 6° for Mach numbers up to 0.96 and approached 15° at the highest Mach number. These values may also be considered to be total aileron deflection inasmuch as the rolling effectiveness of reference 9 was essentially linear through positive and negative aileron deflections at least up to 10°.

Yawing-moment coefficient.- At low angles of attack, considerable favorable yaw was indicated which tended to increase somewhat with Mach number, but to decrease with angle of attack (figs. 7(d) and 9(b)).

Side-force coefficient.- The differential tail produced a positive side force at all angles of attack and Mach numbers of the present tests (figs. 7(e) and 9(c)). The side force decreased, however, with angle of attack in the same manner as the corresponding yawing moment.

Other coefficients.- Figure 7(a) shows that deflecting the horizontal-tail surfaces differentially generally decreased the value of lift coefficient developed at a given angle of attack, particularly at the lower Mach numbers, with little or no change in the initial lift-curve slope.

Deflecting the horizontal-tail surfaces differentially increased significantly the value of drag coefficient over that of the symmetrically deflected model (fig. 8(a)). The drag-coefficient rise was approximately 0.01 and remained essentially constant throughout the angle-of-attack range at all Mach numbers.

There was no significant change in longitudinal stability (figs. 7(b) and 8(b)), although the results indicate the model trimmed at slightly lower lift coefficients for the differentially deflected configuration.

Effects of the Vertical Tail

Figures 7 through 9 also present the effect of the vertical tail on the aerodynamic characteristics of the model with differentially deflected horizontal-tail surfaces. Since for the present tests the left-half section of the horizontal tail was deflected nose down and the right-half section was deflected nose up, the loads on the vertical tail would be expected to be positive on the left side and negative on the right side, producing positive incremental side forces and negative incremental yawing moments. The results of the present tests for the vertical tail-on configuration, which show a positive shift in the side forces (figs. 7(e) and 9(c)) and a negative shift in the corresponding yawing moments (figs. 7(d) and 9(b)) compared to the vertical tail-off configuration, indicate that the expected loads on the vertical tail were realized. Such loads on the vertical tail would also be expected to produce positive incremental rolling moments which, for the present model, would decrease the negative rolling moment produced by the differentially deflected horizontal tail. The results, however, show generally negligible changes in rolling moment (figs. 7(c) and 9(a)) which indicate that the positive rolling moment produced by the loads on the vertical tail were cancelled by the simultaneously increased rolling effectiveness of the differentially deflected horizontal tail or that the center of pressure of the loads on the vertical tail was located very near the horizontal axis of the model.

The positive pitching moment for the differentially deflected tail model is shown to be reduced by the addition of the vertical tail at low angles of attack throughout the Mach number range (figs. 7(b) and 8(b)) which indicated that the vertical tail increased the negative pressures more than the positive pressures on the upper surfaces of the aft portion of the model.

Figure 7(a) shows little, or no, effect on the lift coefficient due to the vertical tail throughout the Mach number and angle-of-attack ranges of the present tests. Figure 8(a) shows an increase in the drag coefficient of about 0.002 due to the vertical tail which was essentially constant throughout the tests. This value was about twice the expected increase in drag coefficient due to skin friction.

It should be added at this point that, in the absence of simultaneously obtained pressure data, the aforementioned analysis of the effects of the vertical tail on the rolling moment and pitching moment is based primarily on deduction. A complete understanding of the influence of the vertical tail on lateral characteristics would require further study.

CONCLUSIONS

Results of an investigation to determine the applicability of differentially deflected horizontal-tail surfaces as high-speed lateral-control devices lead to the following conclusions:

1. The effectiveness as a lateral-control device of a horizontal tail deflected differentially from a constant mean angle of incidence was found to be constant or to increase slightly with Mach number up to a Mach number of 1.05 for angles of attack up to 20°.

2. The rolling-moment effectiveness for the differentially deflected horizontal tail compared with that for a single 0.43-semispan, 30-percent-chord outboard aileron deflected to approximately 6° on a geometrically similar wing for Mach numbers up to 0.96 and to as high as 15° for Mach numbers between 0.96 and 1.05.

3. The differentially deflected horizontal tail produced considerable favorable yawing moment which decreased appreciably with angle of attack at all Mach numbers of the tests.

4. With the horizontal tail deflected differentially, the addition of the vertical tail increased the side force and yawing moment and had little or no effect on rolling moment.

5. The drag increment due to control by differential deflection of the horizontal tail was essentially constant with angle of attack and Mach number at a value of approximately 0.01.

Langley Aeronautical Laboratory,
    National Advisory Committee for Aeronautics,
        Langley Field, Va., September 9, 1955.

REFERENCES

1. West, F. E., Jr., Solomon, William, and Brummal, Edward M.: Investi-
   gation of Spoiler Ailerons With and Without a Gap Behind the Spoiler
   on a 45° Sweptback Wing-Fuselage Combination at Mach Numbers From
   0.60 to 1.03. NACA RM L53G07a, 1953.

2. Vogler, Raymond D.: Wind-Tunnel Investigation at High Subsonic Speeds
   of a Spoiler-Slot-Deflector Combination on an NACA 65A006 Wing With
   Quarter-Chord Line Sweptback 32.6°. NACA RM L53D17, 1953.

3. Tinling, Bruce E., and Karpen, A. V.: The Effects of Trailing-Edge
   Flaps on the Subsonic Aerodynamic Characteristics of an Airplane
   Model Having a Triangular Wing of Aspect Ratio 3. NACA RM A54L07,
   1955.

4. Koenig, David G.: Tests in the Ames 40- by 80-Foot Wind Tunnel of
   an Airplane Configuration With an Aspect Ratio 3, Triangular Wing
   and an All-Movable Horizontal Tail - Longitudinal and Lateral
   Characteristics. NACA RM A52L15, 1953.

5. English, Roland D.: Free-Flight Investigation, Including Some
   Effects of Wing Aeroelasticity, of the Rolling Effectiveness of an
   All-Movable Horizontal Tail With Differential Incidence at Mach
   Numbers From 0.6 to 1.5. NACA RM L54K30, 1954.

6. Ward, Vernon G., Whitcomb, Charles F., and Pearson, Merwin D.: Air-
   Flow and Power Characteristics of the Langley 16-Foot Transonic
   Tunnel With Slotted Test Section. NACA RM L52E01, 1952.

7. Hallissy, Joseph M., and Bowman, Donald R.: Transonic Characteristics
   of a 45° Sweptback Wing-Fuselage Combination. Effect of Longitudinal
   Wing Position and Division of Wing and Fuselage Forces and Moments.
   NACA RM L52K04, 1953.

8. Cahill, Jones F., and Gottlieb, Stanley M.: Low-Speed Aerodynamic
   Characteristics of a Series of Swept Wings Having NACA 65A006 Air-
   foil Sections (Revised). NACA RM L50F16, 1950.

9. Vogler, Raymond D.: Lateral-Control Investigation of Flap-Type Con-
   trols on a Wing With Quarter-Chord Line Swept Back 45°, Aspect
   Ratio 4, Taper Ratio 0.6, and NACA 65A006 Airfoil Section.
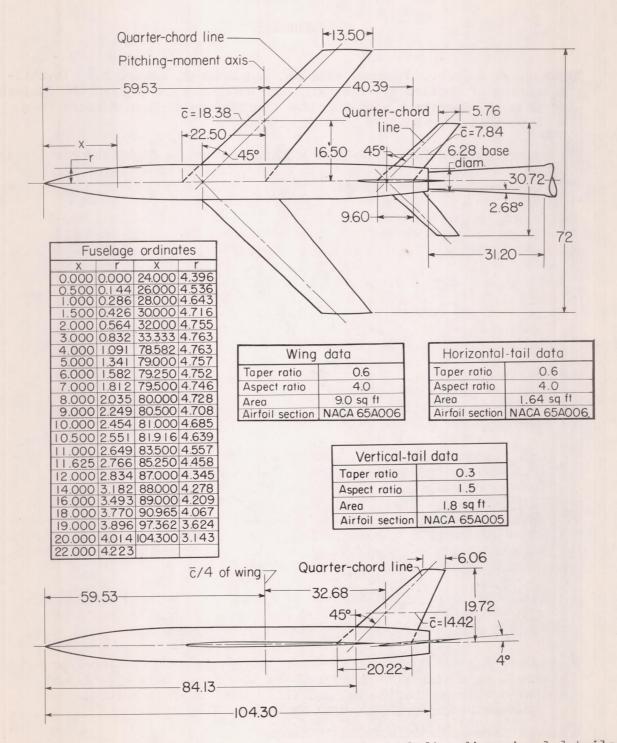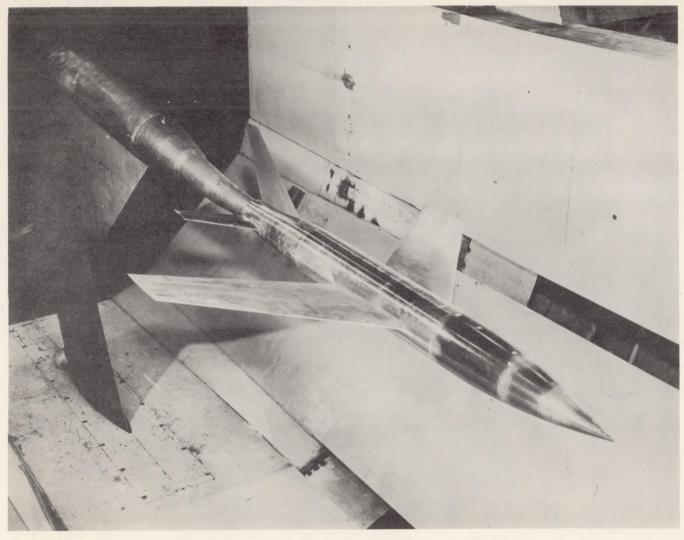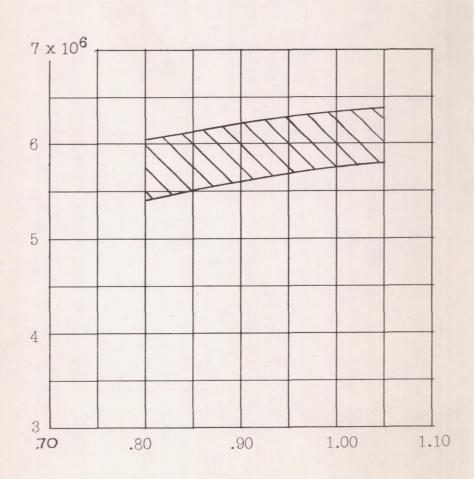   Transonic-Bump Method. NACA RM L9F29a, 1949.

Quarter-chord line

Pitching-moment axis

|←13.50→|

59.53 40.39

$\bar{c}=18.38$ Quarter-chord |← 5.76
line

|←22.50 $\bar{c}=7.84$

45° 16.50 45° 6.28 base
diam.

x 30.72

r 2.68°

9.60 31.20

72

Fuselage ordinates			
x	r	x	r
0.000	0.000	24.000	4.396
0.500	0.144	26.000	4.536
1.000	0.286	28.000	4.643
1.500	0.426	30.000	4.716
2.000	0.564	32.000	4.755
3.000	0.832	33.333	4.763
4.000	1.091	78.582	4.763
5.000	1.341	79.000	4.757
6.000	1.582	79.250	4.752
7.000	1.812	79.500	4.746
8.000	2.035	80.000	4.728
9.000	2.249	80.500	4.708
10.000	2.454	81.000	4.685
10.500	2.551	81.916	4.639
11.000	2.649	83.500	4.557
11.625	2.766	85.250	4.458
12.000	2.834	87.000	4.345
14.000	3.182	88.000	4.278
16.000	3.493	89.000	4.209
18.000	3.770	90.965	4.067
19.000	3.896	97.362	3.624
20.000	4.014	104.300	3.143
22.000	4.223		

Wing data	
Taper ratio	0.6
Aspect ratio	4.0
Area	9.0 sq ft
Airfoil section	NACA 65A006

Horizontal-tail data	
Taper ratio	0.6
Aspect ratio	4.0
Area	1.64 sq ft
Airfoil section	NACA 65A006

Vertical-tail data	
Taper ratio	0.3
Aspect ratio	1.5
Area	1.8 sq ft
Airfoil section	NACA 65A005

$\bar{c}/4$ of wing Quarter-chord line |← 6.06

59.53 32.68

45° 19.72

$\bar{c}=14.42$

20.22

84.13 4°

104.30

Figure 1.- Diagram of the model configuration including dimensional details
of the horizontal- and vertical-tail surfaces. All linear dimensions
are in inches.

L-88814
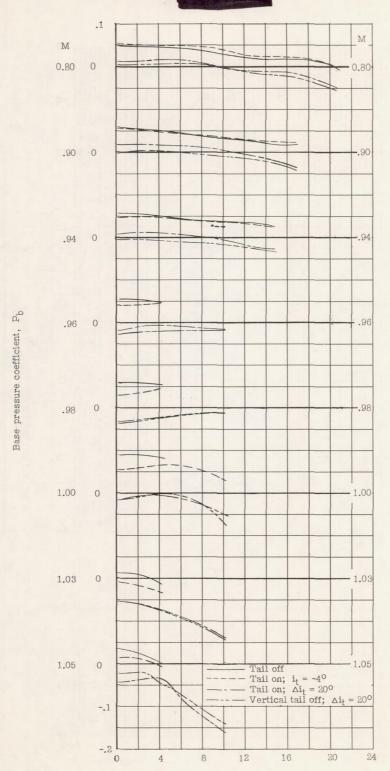
Figure 2.- Model and sting-support system in the Langley 16-foot transonic tunnel.
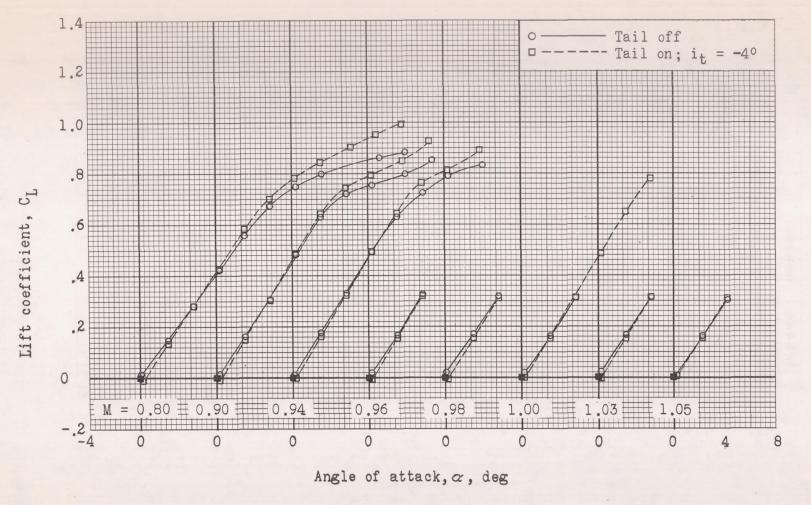
Figure 3.- Variation of Reynolds number (based on mean aerodynamic chord) with Mach number.

Figure 4.- Variation of average base-pressure coefficient with angle of attack for all configurations.

Tail off
Tail on; $i_t = -4°$

1.4

1.2

1.0

.8

.6

.4

.2

0

-.2

Lift coefficient, C_L

M = 0.80   0.90   0.94   0.96   0.98   1.00   1.03   1.05

-4   0   0   0   0   0   0   0   0   4   8

Angle of attack, α, deg
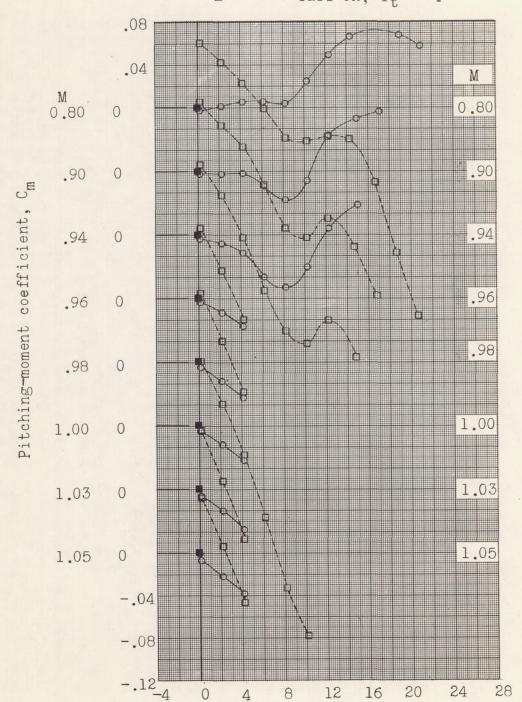
(a) Lift coefficient.

Figure 5.- Variation with angle of attack of the aerodynamic character-
istics for the basic tail-off model and for the symmetrical
horizontal-tail configuration.
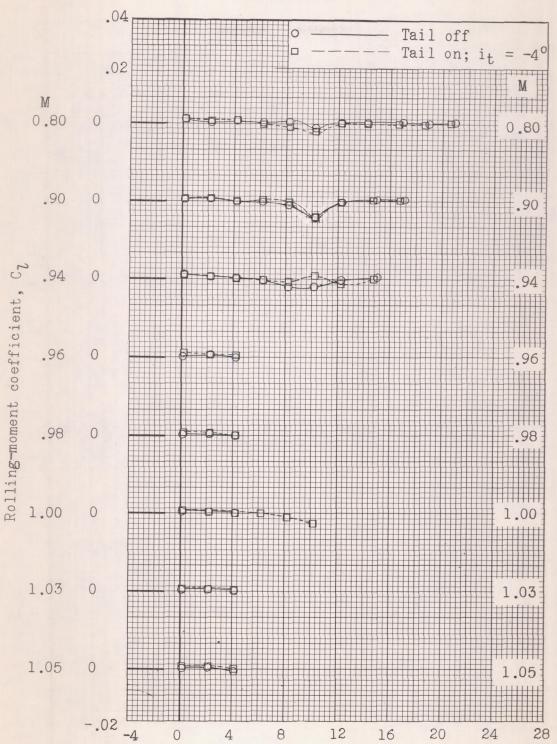
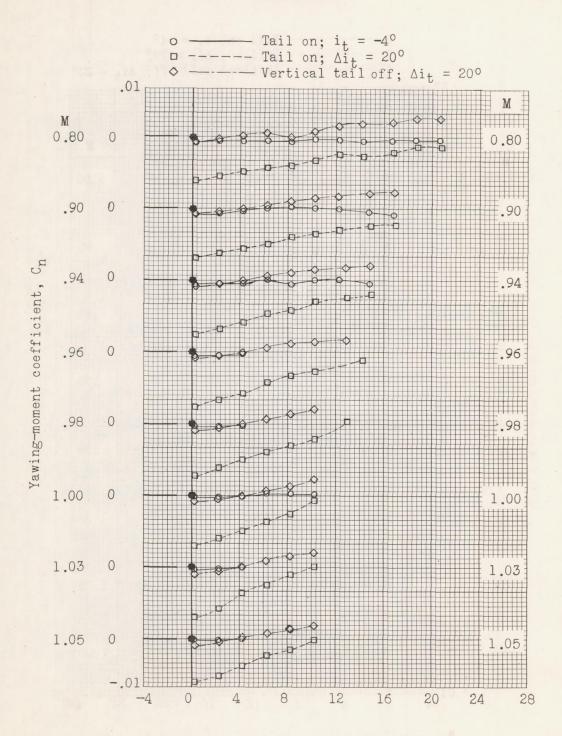Angle of attack, α, deg

(b) Pitching-moment coefficient.

Figure 5.- Continued.

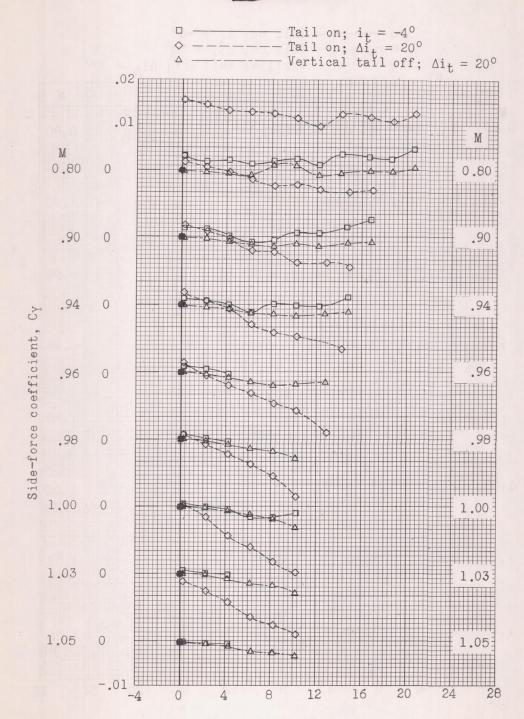(c) Rolling-moment coefficient.

Figure 5.- Continued.

Angle of attack, α, deg
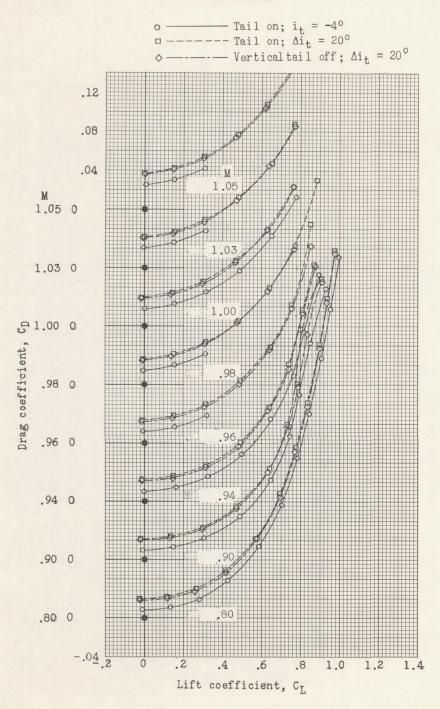
(d) Yawing-moment coefficient.

Figure 5.- Continued.

Angle of attack, α, deg

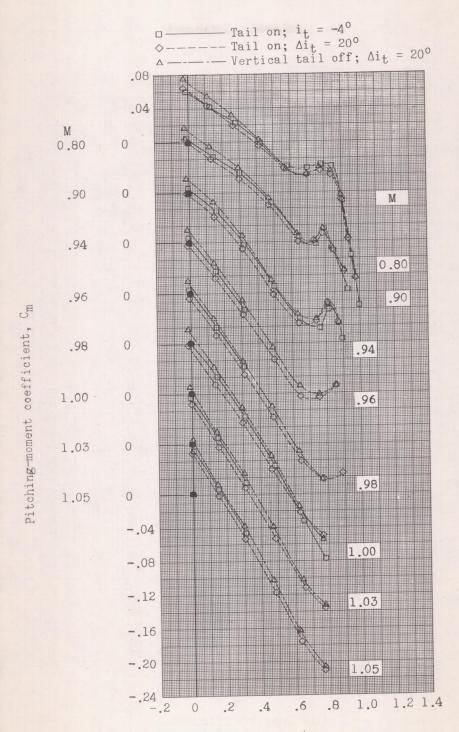(e) Side-force coefficient.

Figure 5.- Concluded.

CONFIDENTIAL
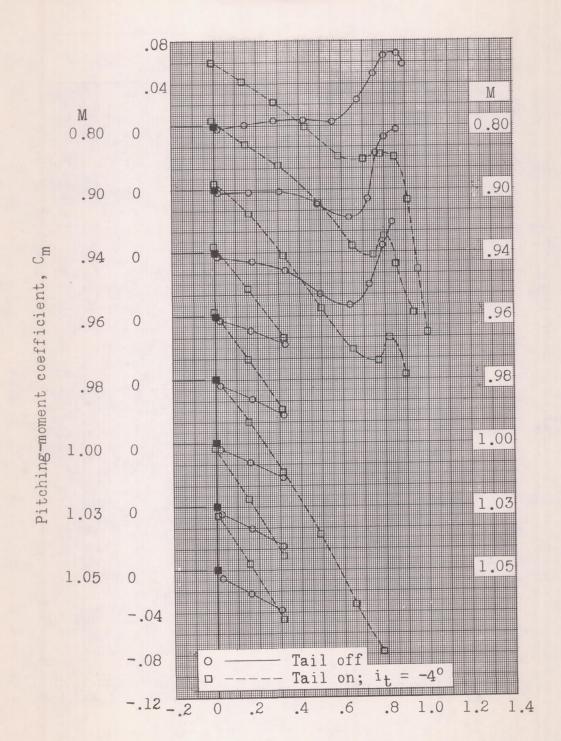
(a) Drag coefficient.

Figure 6.- Variation with lift coefficient of the drag, pitching-moment, and rolling-moment coefficients for the basic tail-off model and for the symmetrical horizontal-tail configuration.

CONFIDENTIAL
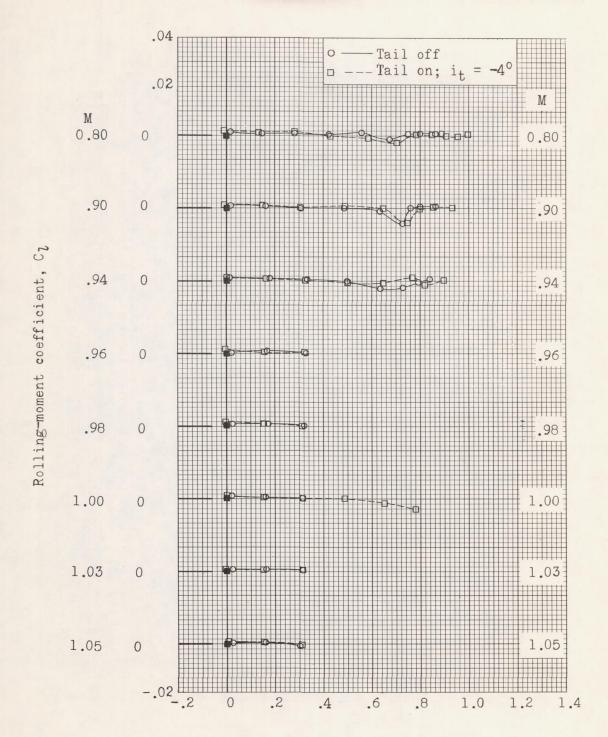
Lift coefficient, C_L

(b) Pitching-moment coefficient.

Figure 6.- Continued.

CONFIDENTIAL

Lift coefficient, C_L
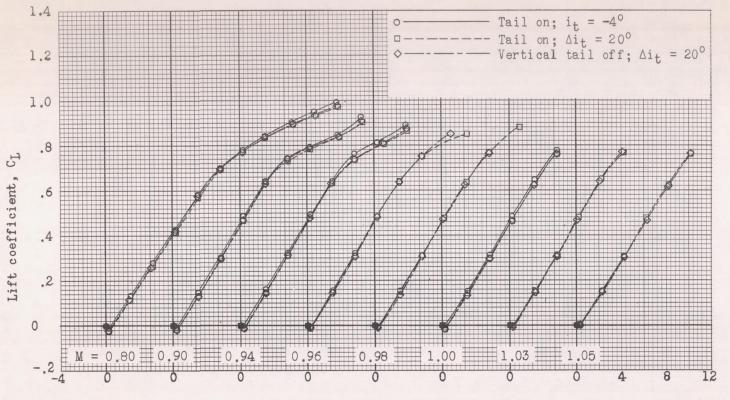
(c) Rolling-moment coefficient.

Figure 6.- Concluded.
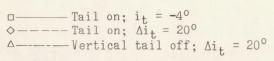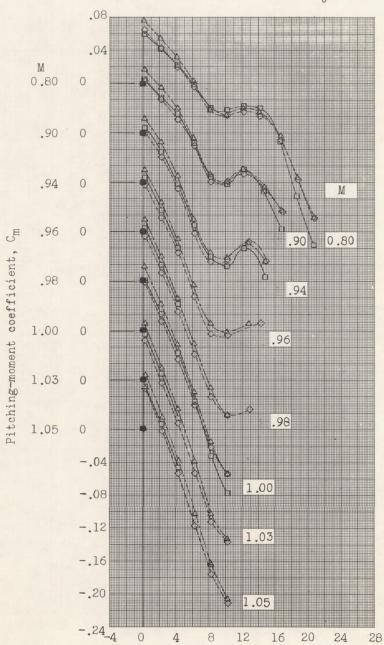
(a) Lift coefficient.

Figure 7.- Variation with angle of attack of the aerodynamic charac-
teristics for the symmetrical horizontal-tail configuration and for
the differentially deflected horizontal-tail configuration with and
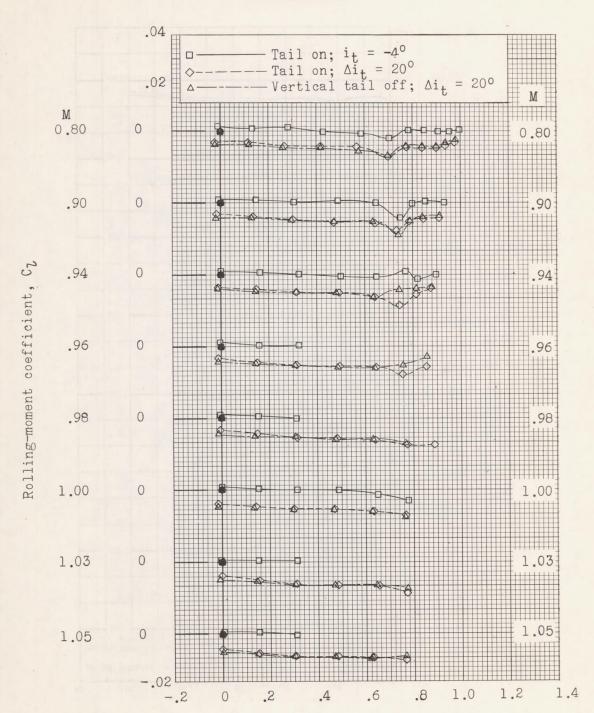without the vertical tail.
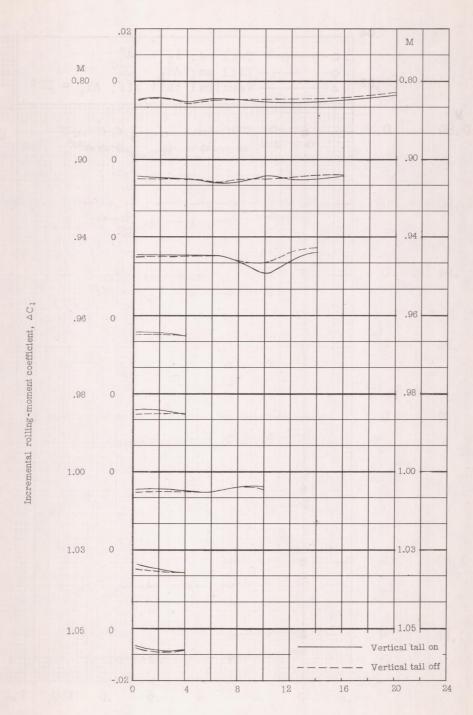
(b) Pitching-moment coefficient.

Figure 7.- Continued.

Angle of attack, α, deg

(c) Rolling-moment coefficient.

Figure 7.- Continued.

Angle of attack, α, deg

(d) Yawing-moment coefficient.

Figure 7.- Continued.

CONFIDENTIAL

Angle of attack, α, deg

(e) Side-force coefficient.

Figure 7.- Concluded.

CONFIDENTIAL

(a) Drag coefficient.

Figure 8.- Variation with lift coefficient of the drag, pitching-moment, and rolling-moment coefficients for the symmetrical horizontal-tail configuration and for the differentially deflected horizontal-tail configuration with and without the vertical tail.

(b) Pitching-moment coefficient.

Figure 8.- Continued.

Lift coefficient, C_L

(c) Rolling-moment coefficient.

Figure 8.- Concluded.
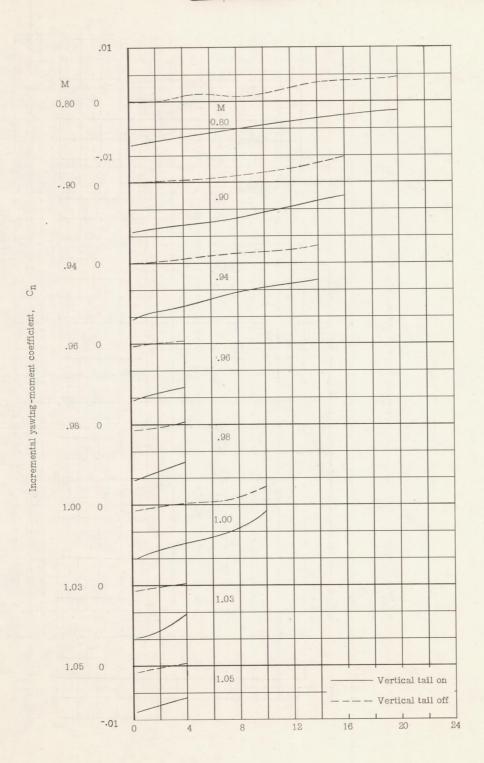
(a) Incremental rolling-moment coefficient.

Figure 9.- Incremental rolling-moment, yawing-moment, and side-force
   coefficients due to differential deflection of the horizontal-tail
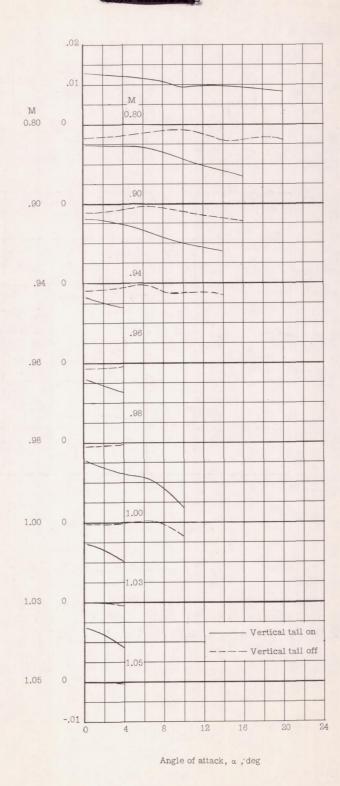   surfaces with and without the vertical tail.

(b) Incremental yawing-moment coefficient.
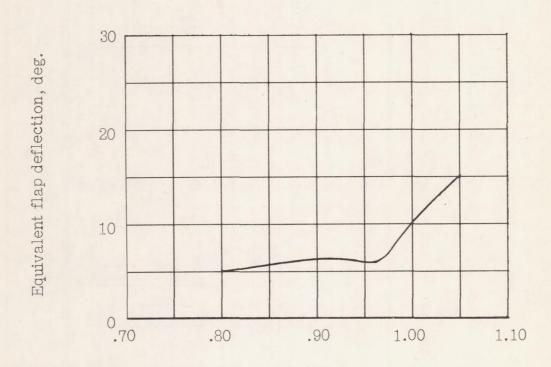
Figure 9.- Continued.
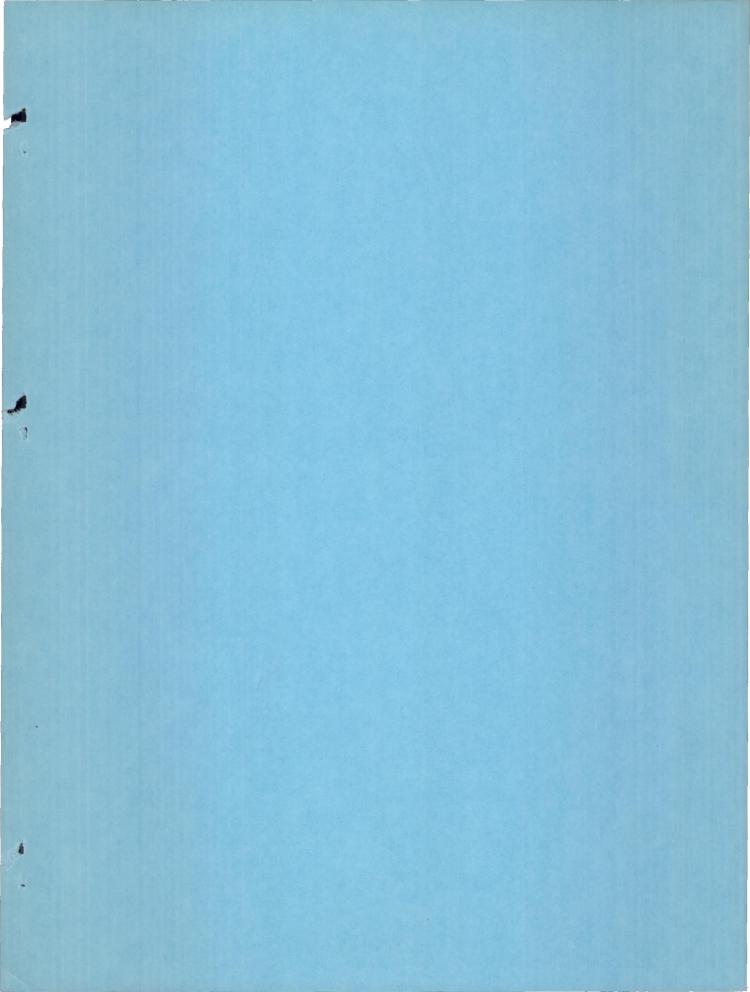
(c) Incremental side-force coefficient.

Figure 9.- Concluded.

Mach number, M

Figure 10.- Approximate deflection of a single 30-percent-chord flap-
type aileron required to produce the same rolling moment as the
differentially deflected horizontal tail at $\Delta i_t = 20^\circ$ and $\alpha = 2^\circ$.